ON THE USE OF NEW ADAPTIVE SUBBAND STRUCTURES IN ACOUSTIC ECHO CANCELLATION

Mariane R. Petraglia† mariane@coe.ufrj.br

Rogerio G. Alves†‡ guedes@lps.ufrj.br

Antonio Petraglia† antonio@coe.ufrj.br

†Federal University of Rio de Janeiro
COPPE – Program of Electrical Engineering
CP 68564, CEP 21945 970
Rio de Janeiro, RJ – Brazil

‡INMETRO – National Institute of Metrology
DIMCI/DIELE/LATCE
CP 94501, CEP 25250 020
Duque de Caxias, RJ – Brazil

ABSTRACT

A new family of adaptive structures which employ filter banks or wavelets to decompose the input signal and reduced-order adaptive filters in the subbands is applied to the acoustic echo control problem. Structures with sparse adaptive subfilters and no down-sampling of the subband signals, as well as structures with critical sampling of the subband signals, are investigated. Both types of structures yield exact modeling of FIR systems. Computer simulations are presented to illustrate the convergence behavior of the adaptive subband structures investigated in the paper for acoustic echo cancellation.

1 INTRODUCTION

Adaptive FIR filters have been extensively used in acoustic echo control, as reported in [1]-[3]. Due to the nature of the problem, large order adaptive filters are usually required in order to cancel out a large amount of echo contained in the received signal. In such applications, the conventional adaptive FIR algorithms present several drawbacks, such as the large number of operations needed for their implementation and slow convergence. Alternative structures that make use of transforms and filter banks have been proposed [2]-[6] with the objective of reducing the drawbacks described above. In [4], a transform was applied to the input vector and sparse adaptive subfilters were used in the subbands. In [5],[6], analysis filters (instead of transforms) were used, resulting in the general structure of Fig. 1(a). The better selectivity of the filter banks when compared to a transform-based bank can lead to significant reduction in the convergence time for colored input signals.

The structure of Fig. 1(a) was believed until recently of being able to implement only a subclass of FIR systems, due to the length of the filter realized being larger than the number of adaptive coefficients [6]. In [7], it was shown that by properly choosing the filter bank and the number of coefficients of the adaptive subfilters, the structure of Fig. 1(a) becomes capable of modeling any FIR system, with the introduction of a small delay which is inherent to the filter bank.

The results obtained for the structure of Fig. 1(a) can be extended to the case where non-uniform filter banks or wavelets are used to decompose the input signal. The adaptive subfilters of the resulting structure present different lengths and sparsity factors. The coefficients of the subfilters are adapted by an LMS-type algorithm, where the step-size for each subfilter is normalized by an estimate of the power of the respective subband signal. For colored input signals, such power normalization can reduce significantly the eigenvalue spread of the overall auto-correlation matrix, resulting in better convergence rates than the conventional LMS algorithm, specially for large order filters.

From the filter bank adaptive structure with sparse subfilters, a new family of adaptive structures with critical sampling of the subband signals, which also yield exact modeling of FIR systems, can be obtained [7]. The resulting structures present extra filters between the subbands, but such filters are related to the direct-path adaptive filters, and do not need to be adapted separately. Therefore, the computational complexity is reduced and the adaptation speed is improved when compared to the algorithms derived in [2].

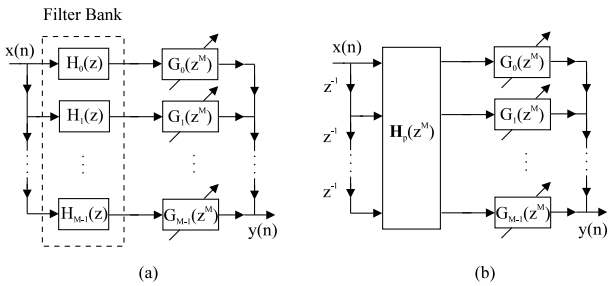

Figure 1: Adaptive structure using an analysis filter bank and sparse subfilters.

2 ADAPTIVE FILTER BANK STRUCTURE WITH SPARSE FILTERS

Let us consider initially the structure of Fig. 1(a) with two subbands ($M = 2$), which can be represented as in Fig. 1(b) by making use of the polyphase matrix of the

analysis filter bank [8], i.e.,

$$\boldsymbol{H}_p(z) = \begin{bmatrix} H_{0,0}(z) & H_{0,1}(z) \\ H_{1,0}(z) & H_{1,1}(z) \end{bmatrix}, \quad (1)$$

where $H_{i,j}(z)$ is the jth component of the type-1 polyphase decomposition of the analysis filter $H_i(z) = \sum_{n=0}^{N_{H_i}} h_i(n) z^{-n}$.

The transfer function implemented by the adaptive structure of Fig. 1(b) is given by

$$H(z) = \begin{bmatrix} G_0(z^2) & G_1(z^2) \end{bmatrix} \boldsymbol{H}_p(z^2) \begin{bmatrix} 1 \\ z^{-1} \end{bmatrix}. \quad (2)$$

In a system identification application, the coefficients of the subfilters $G_i(z^2)$ are adapted such as to model an unknown FIR system, which will be denoted here by $P(z)$. The type-1 polyphase decomposition of the transfer function of the unknown system is given by

$$\begin{aligned} P(z) &= P_0(z^2) + z^{-1} P_1(z^2) = \\ &= \begin{bmatrix} P_0(z^2) & P_1(z^2) \end{bmatrix} \begin{bmatrix} 1 \\ z^{-1} \end{bmatrix}. \end{aligned} \quad (3)$$

From the two equations above, we observe that the subband structure will model exactly the unknown FIR system when

$$\begin{bmatrix} G_0(z^2) & G_1(z^2) \end{bmatrix} \boldsymbol{H}_p(z^2) = \begin{bmatrix} P_0(z^2) & P_1(z^2) \end{bmatrix}. \quad (4)$$

Such equality can not be achieved, since for adaptive subfilters with K coefficients and analysis filters of length N_H the products $G_i(z^2) H_{i,j}(z^2)$ will have lengths $2K + N_H - 1$, which are larger than the number of coefficients $2K$ being adapted. However, if we allow the introduction of a constant delay of Δ samples at the output, we can have

$$\begin{bmatrix} G_0(z^2) & G_1(z^2) \end{bmatrix} \boldsymbol{H}_p(z^2) = \begin{bmatrix} P_0(z^2) & P_1(z^2) \end{bmatrix} z^{-\Delta}, \quad (5)$$

if

$$\begin{bmatrix} G_0(z^2) & G_1(z^2) \end{bmatrix} = \begin{bmatrix} P_0(z^2) & P_1(z^2) \end{bmatrix} \boldsymbol{F}_p(z^2), \quad (6)$$

such that $\boldsymbol{F}_p(z^2) \boldsymbol{H}_p(z^2) = z^{-\Delta} \boldsymbol{I}$, where $\boldsymbol{I}$ is the 2×2 identity matrix. The matrices $\boldsymbol{H}_p(z)$ and $\boldsymbol{F}_p(z)$ that satisfy the above condition correspond to the polyphase matrices of the analysis and synthesis filter banks of a perfect reconstruction multirate system. The polyphase matrix of the synthesis bank

$$\boldsymbol{F}_p(z) = \begin{bmatrix} F_{0,0}(z) & F_{1,0}(z) \\ F_{0,1}(z) & F_{1,1}(z) \end{bmatrix} \quad (7)$$

is such that $F_{i,j}(z)$ is the jth component of the type-2 polyphase decomposition of the synthesis filter $F_i(z) = \sum_{n=0}^{N_{F_i}} f_i(n) z^{-n}$ [8].

Therefore, by using an analysis filter bank which yields perfect reconstruction and adaptive subfilters of sufficient order such that Eq. (6) can be achieved, the structure of Fig. 1(a) implements exactly any FIR system. It should be emphasized that in the adaptation algorithm the delay introduced by the filter banks must be taken into account.

We can extend the two-channel structure for a multichannel tree structure, by implementing any of the sparse adaptive subfilters $G_i(z^2)$ using a two-channel adaptive subband structure. Particular cases of the resulting filter banks correspond to discrete wavelets [8]. In this way, we generalize the two-channel subband structure to an adaptive structure with any number of channels, where the adaptive subfilters migth have now different sparsity factors M_i. The resulting multichannel adaptive structure is much more versatile than the other transform-domain and frequency-domain algorithms, since it allows the use of a number of subbands different from the number of coefficients, frequency decomposition of the input signals with different frequency bandwidths, and adaptive subfilters of different lengths and sparsities for the different subbands. The number of adaptive coefficients of each subfilter $G_i(z^{M_i})$ should be at least

$$K_i = \lfloor N/M_i \rfloor + \lfloor N_{F_i}/M_i \rfloor + 1, \quad (8)$$

where N is the order of the unknown system, N_{F_i} is the order of the synthesis filter of the i-th band, and M_i is the sparsity factor of the corresponding subfilter.

2.1 Adaptation Algorithm

Denoting $x_i(n)$ the signal at the output of the ith analysis filter, $g_{i,k}$ the k-th coefficient of the subfilter $G_i(z)$ and K_i the corresponding number of coefficients, the general form for the LMS adaptation algorithm that minimizes the overall mean-square error $e(n)$ is

$$g_{i,k}(n) = g_{i,k}(n-1) + \mu_i(n) e(n) x_i(n - M_i k), \quad (9)$$

for $i = 0, 1, \cdots, M-1$ and $k = 0, 1, \cdots, K_i - 1$, where M is the number of subbands. The step-sizes are given by

$$\mu_i(n) = \frac{\mu}{\sum_{k=0}^{K_i - 1} x_i(n - M_i k)^2 + c} \quad (10)$$

where c is a small constant which prevents the algorithm from diverging when the power of $x_i(n)$ is very small. The use of different step-sizes in the adaptation of the coefficients of the different subfilters, according to (10), increases significantly the convergence speed of the adaptive algorithm for colored input signals when compared to the speed of the conventional LMS algorithm.

3 ADAPTIVE SUBBAND STRUCTURE WITH CRITICAL SAMPLING

Now, by including maximally decimated perfect reconstruction analysis and synthesis banks following each

sparse subfilter in Fig. 1(a), moving the sparse subfilters $G_k(z^M)$ to the right of the decimators (becoming thus $G_k(z)$ by the *noble identity* [8]), and assuming that non-adjacent filters of the analysis filter bank have frequency responses which do not overlap, the structure of Fig. 2 is obtained. Observe that in the resulting structure only M subfilters need to be adapted, namely $G_0(z), \cdots, G_{M-1}(z)$, and that they operate at a rate which is $1/M$-th of the input rate.

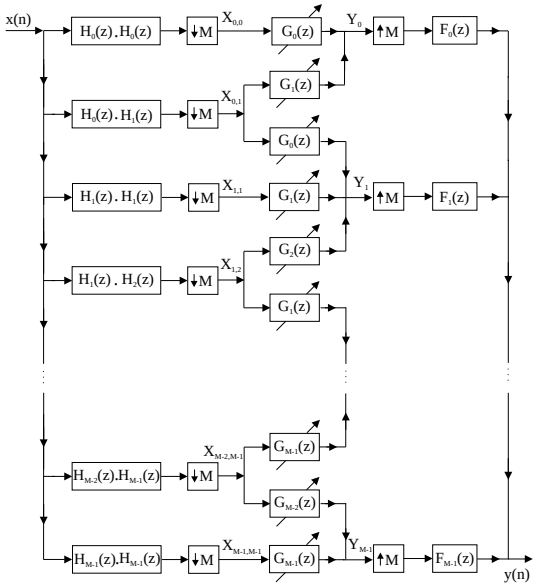

Figure 2: Adaptive subband structure with critical subsampling.

3.1 Adaptation Algorithm

The major advantage of the subband structure of Fig. 2 is that, for an M-subband scheme, only M subfilters need to be adapted, as opposed to the overdetermined method presented in [2], where $3M-2$ subfilters are adapted. Moreover, the structure of Fig. 2 presents the advantage that the subfilters are adapted separately, as opposed to the nonoverdetermined method also described in [2], which updates a single filter and then derives the coefficients of the subfilters.

A normalized LMS-type algorithm is used for updating the coefficients of the subfilters. Denoting $\boldsymbol{X}_{i,j}(m)$ the vector containing the actual plus $K-1$ past samples of the signal $X_{i,j}$ at the output of the analysis filter $H_i(z)H_j(z)$ after down-sampling (see Fig. 2), $\boldsymbol{G}_i(m)$ the vector containing the coefficients of the subfilter $G_i(z)$ at iteration m, and K the number of coefficients of each subfilter, the general form for the LMS adaptation algorithm that minimizes the sum of the instantaneous subband squared-errors is given by

$$\boldsymbol{G}_k(m+1) = \boldsymbol{G}_k(m) + \mu_k(m)[\boldsymbol{X}_{k,k}(m)E_k(m) + \boldsymbol{X}_{k-1,k}(m)E_{k-1}(m) + \boldsymbol{X}_{k,k+1}(m)E_{k+1}(m)], \quad (11)$$

where the error signal $E_k(m)$ is

$$E_k(m) = D_k(m-\Delta/M) - [\boldsymbol{X}_{k,k}(m)^T\boldsymbol{G}_k(m) + \boldsymbol{X}_{k-1,k}(m)^T\boldsymbol{G}_{k-1}(m) + \boldsymbol{X}_{k,k+1}(m)^T\boldsymbol{G}_{k+1}(m)]. \quad (12)$$

For the first and last subbands ($k=0$ and $k=M-1$) one should consider $\boldsymbol{X}_{-1,0} = \mathbf{0}$ and $\boldsymbol{X}_{M-1,M} = \mathbf{0}$. The step-sizes are made inversely proportional to the sum of the powers of the signals involved in the adaptation of the coefficients, that is

$$\mu_k(m) = \frac{\mu}{|\boldsymbol{X}_{k,k}(m)|^2 + |\boldsymbol{X}_{k-1,k}(m)|^2 + |\boldsymbol{X}_{k,k+1}(m)|^2 + c}. \quad (13)$$

4 COMPUTER SIMULATIONS

Computer simulations are presented in this section to illustrate the convergence behavior of both types of subband structures described in this paper for acoustic echo cancelling applications. The tests were performed using the measured impulse response of the echo path in an automobile and speech signals sampled at a rate of 8 KHz. The echo path was modeled by a 256-length FIR adaptive filter (N=255).

4.1 Sparse Filter Bank Structure

The adaptive filter bank structure with sparse subfilters was simulated with two, four, and eight subbands, and with the analysis bank implemented by a tree-structure with prototype filters given by $H^{(0)}(z) = \frac{1}{8}(-1+2z^{-1}+6z^{-2}+2z^{-3}-z^{-4})$ and $H^{(1)}(z) = \frac{1}{2}(-1+2z^{-1}-z^{-2})$, which leads to perfect reconstruction filter banks. The number of adaptive coefficients in each subfilter was set according to Eq. (8). The step-size normalization of Eq. (10) was implemented with $\mu = 0.5$ for all simulations.

Figure 3 presents the normalized Euclidean norm of the difference between the adaptive weights and the echo path impulse response for the normalized LMS algorithm and for the sparse filter bank structure with $M=2$, $M=4$, and $M=8$ subbands. We observe that the convergence rate improves with the increase of the number of subbands, as expected. However, the input-output delay introduced by the structure also increases ($\Delta = 2$ for $M=2$, $\Delta = 6$ for $M=4$, and $\Delta = 14$ for $M=8$), as well as its computational complexity. Such increases are significant only when the number of subbands is very large or when more selective analysis filters are used. We have also performed simulations with wavelet-type tree structures, where only the low-pass subbands were further decomposed. The convergence speed obtained using a wavelet was exactly the same as that of the complete tree-structure, and the computational complexity was smaller.

4.2 Critically Sampled Subband Structure

The adaptive subband structure of Fig. 2 was implemented with two, four and eight subbands, and with

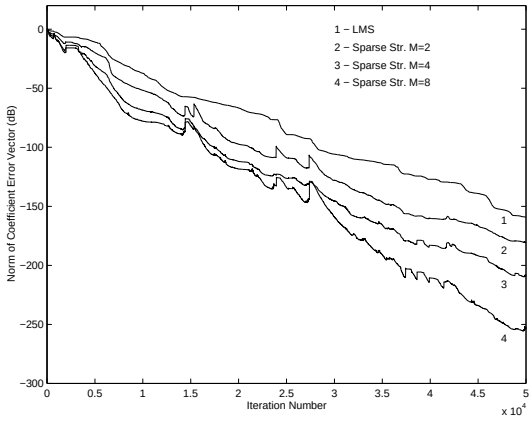

Figure 3: Simulation results for the sparse filter bank structure.

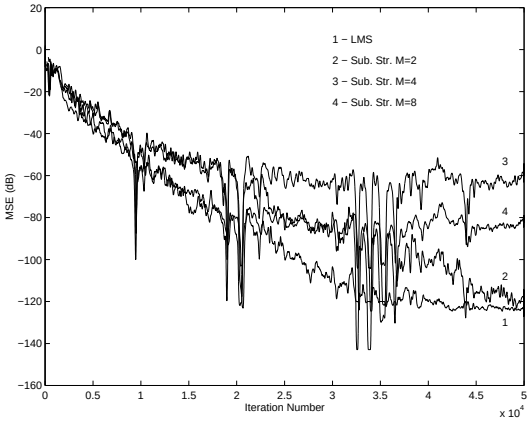

Figure 4: Simulation results for the critically sampled subband structure.

perfect reconstruction cosine modulated analysis and synthesis banks [8]. The orders of the prototype filters were $N_F = 23$ for $M = 2$, $N_F = 47$ for $M = 4$, and $N_F = 127$ for $M = 8$. The number of coefficients of each subfilter was $K = (N + N_F + 2)/M$. The step-sizes were normalized according to Eq. (13) with $\mu = 1/1.5$.

Figure 4 presents the MSE evolution for the critically subband structures with $M = 2$, $M = 4$, and $M = 8$, and for the normalized LMS algorithm. We observe that the convergence speeds of the subband structure and of the LMS algorithm are practically the same, due to the adaptation at the lower rate in the subband structure. The final MSE of the subband structure is limited by the stopband attenuation of the analysis filters when $M > 2$, since we have assumed in the derivation of the structure and of the adaptive algorithm that the frequency responses of non-adjacent filters do not overlap. The main advantage of the critically sampled subband structure is the savings in the computational complexity, which is of the order of the number of subbands M, for N large. However the delay introduced by this structure is larger than that of the sparse structure, and it increases with the number of subbands and the order of the analysis and synthesis filters.

5 CONCLUSIONS

A new family of adaptive subband structures was applied to the acoustic echo cancellation problem. Simulations with the adaptive subband structure with sparse subfilters have shown that a significant improvement can be obtained even when very simple filter banks or wavelets and few subbands are used. For the subband structure with critical sampling, the convergence speed of the adaptation algorithm is almost the same as that of the full-band LMS algorithm, and it results in computational complexity reduction when implementing high-order adaptive filters. However, the increase in the number of subbands leads to an increase in the input-output delay introduced by the filter banks.

References

[1] E. Haensler, "The hands-free telephone problem - An annotated bibliography," *Signal Processing*, pp. 259-271, vol. 27, Jun. 1992.

[2] A. Gilloire and M. Vetterli, "Adaptive filtering in subbands with critical sampling: analysis, experiments, and application to acoustic echo cancellation," *IEEE Trans. Signal Processing*, pp. 1862-1875, vol. 40, no. 8, Aug. 1992.

[3] M. R. Petraglia and S. K. Mitra, "Performance analysis of adaptive filter structures based on subband decomposition," in *Proc. IEEE Int. Symp. Circ. Syst.*, pp. 60-63, Chicago, IL, May 1993.

[4] M. R. Petraglia and S. K. Mitra,"Adaptive FIR filter structure based on the generalized subband decomposition of FIR filters," *IEEE Transactions on Circuits and Systems II: Analog and Digital Signal Processing*, vol. 40, pp. 354-362, June 1993.

[5] M. R. Petraglia and S. K. Mitra, "An adaptive filter bank structure for adaptive line enhancement and channel equalization applications," in *Proc. SBT/IEEE Int. Telecommunications Symp.*, Rio de Janeiro, Brazil, pp. 1-5, Aug. 1994.

[6] B. E. Usevitch and M. T. Orchard,"Adaptive filtering using filter banks," *IEEE Transactions on Circuits and Systems II: Analog and Digital Signal Processing*, vol. 43, pp. 255-265, March 1996.

[7] M. R. Petraglia, and R. G. Alves, "New Results on Adaptive Filtering Using Filter Banks," *Proc. IEEE Int. Symp. on Circuits and Systems*, pp. 2321-2324, Hong Kong, June 1997.

[8] G. Strang and T. Nguyen, *Wavelets and Filter Banks*. Wellesley - Cambridge Press, 1996.